Society For Biomaterials

Development of novel electrically conductive scaffold based on hyperbranched polyester and polythiophene for tissue engineering applications

Mehdi Jaymand,[1] Raana Sarvari,[2] Parisa Abbaszadeh,[2] Bakhshali Massoumi,[2] Morteza Eskandani,[1] Younes Beygi-Khosrowshahi[3,4]

[1]Research Center for Pharmaceutical Nanotechnology, Tabriz University of Medical Sciences, P.O. Box: 51656-65811, Tabriz, Islamic Republic of Iran
[2]Department of Chemistry, Payame Noor University, P.O. BOX: 19395-3697, Tehran, Islamic Republic of Iran
[3]Stem Cell and Tissue Engineering Research Laboratory, Sahand University of Technology, P.O. Box: 51335-1996, Tabriz, Islamic Republic of Iran
[4]Chemical Engineering Department, Faculty of Engineering, Azarbaijan Shahid Madani University, P.O. Box: 53751-71379, Tabriz, Islamic Republic of Iran

Received 14 January 2016; revised 24 May 2016; accepted 16 June 2016
Published online 4 July 2016 in Wiley Online Library (wileyonlinelibrary.com). DOI: 10.1002/jbm.a.35811

Abstract: A novel electrically conductive scaffold containing hyperbranched aliphatic polyester (HAP), polythiophene (PTh), and poly(ε-caprolactone) (PCL) for regenerative medicine application was succesfully fabricated via electrospinning technique. For this purpose, the HAP (G4; fourth generation) was synthesized via melt polycondensation reaction from *tris*(methylol)propane and 2,2-*bis*(methylol)propionic acid (*bis*-MPA). Afterward, the synthesized HAP was functionalized with 2-thiopheneacetic acid in the presence of *N*,*N*-dicyclohexyl carbodiimide, and *N*-hydroxysuccinimide as coupling agent and catalyst, respectively, to afford a thiophene-functionalized G4 macromonomer. This macromonomer was subsequently used in chemical oxidation copolymerization with thiophene monomer to produce a star-shaped PTh with G4 core (G4-PTh). The solution of the G4-PTh, and PCL was electrospun to produce uniform, conductive, and biocompatible nanofibers. The conductivity, hydrophilicity, and mechanical properties of these nanofibers were investigated. The biocompatibility of the electrospun nanofibers were evaluated by assessing the adhesion and proliferation of mouse osteoblast MC3T3-E1 cell line and *in vitro* degradability to demonstrate their potential uses as a tissue engineering scaffold. © 2016 Wiley Periodicals, Inc. J Biomed Mater Res Part A: 104A: 2673–2684, 2016.

Key Words: polythiophene, electrospinning, conducting scaffold, biocompatibility, tissue engineering

How to cite this article: Jaymand M, Sarvari R, Abbaszadeh P, Massoumi B, Eskandani M, Beygi-Khosrowshahi Y. 2016. Development of novel electrically conductive scaffold based on hyperbranched polyester and polythiophene for tissue engineering applications. J Biomed Mater Res Part A 2016:104A:2673–2684.

INTRODUCTION

The last decade has witnessed the design and development of novel multifunctional materials for application in regeneration/replacement of damaged or diseased tissues by delivering human extracellular matrix (ECM) components (e.g., specialized mediating cytokines and growth factors). Several biological processes such as cell and cell–matrix interactions, external adhesive ligands, superficial structure, and surface topography can affect various cell responses including proliferation, migration, and differentiation.[1–4] On the other hand, it is well established that some biological tissues exhibit electrical activities for modulating cellular fate, processes and behaviors, and electrical stimulation. Thus, a conductive scaffold can promote cell proliferation and differentiation, specifically for neural, cardiac, and muscle tissues. Based on these reasons, the design and development of biodegradable, biocompatible, and electrically conductive polymeric scaffolds is an immensely important in modern regenerative medicine, which has been the subject of intensive research.[5–7] In addition, the scaffolds for regenerative medicine must possess some properties as follows: (1) biocompatibility and biodegradability, (2) suitable microstructures, and mechanical characteristics, (3) proper surface topography and chemical composition, (4) simple and cost-effective fabrication technology.[8–12]

In this respect, the conductive polymers such as polythiophene (PTh), and its derivatives (especially poly(3,4-ethylenedioxythiophene)) have been witnessed an immense interest for the fabrication of conductive scaffolds.[13–16] The PTh and its derivatives are the most important members of

Correspondence to: B. Massoumi; e-mail: b_massoumi@pnu.ac.ir or bakhshalim@yahoo.com

electrically conductive polymers (ECPs) family, due to their importance in basic scientific research, and potential industrial and biomedical applications. This tendency is originated from their unique physicochemical properties, such as excellent environmental and thermal stabilities, high electrical conductivities, mechanical strengths, magnetic and optical properties, ease synthesis, and low costs.[17–22] Despite, incorporating of PTh into the biomedical field remains limited, mainly due to its poor mechanical properties, nondegradability, and difficulty to process into complex three-dimensional structures when used individually.

The synthetic scaffolds can be engineered to possess the desired dimensions, mechanical properties, and degradation profiles through blending or copolymerization of conducting polymer with insulating polymers (generally biocompatible polymers, such as poly(ϵ-caprolactone), poly(ethylene glycol), gelatin, collagen, chitosan, and many more).[10,14,23] In this context, aliphatic polyesters may be an appropriate candidate, because of their biocompatibility, biodegradability, and low costs. Among the aliphatic polyesters, the hyperbranched polyesters based on 2,2-*bis*(methylol)propionic acid have stimulated great interest, mainly due to their highly branched structure and the large number of functional groups, unique physicochemical properties, and significant advantage for industrial and biomedical applications.[24–27]

The electrospinning is suggested as an efficient approach to prepare biocompatible conductive nanofibers to mimic the architecture and biological functions of the ECM. This technique has attracted a great deal of attention in the past decade for fabrication of conductive scaffolds, mainly due to high porosity, high surface-to-volume ratio, ultrathin continuous fibers, adjustable pore size distribution as well as its simplicity and more cost-effectivity.[29,30]

The objective of the present study is to fabrication of novel three-dimensional (3D), conducting, biocompatible, and porous scaffold composed of hyperbranched aliphatic polyester (HAP), polythiophene (PTh), and poly(ϵ-caprolactone) (PCL) for tissue engineering applications. The morphology, electerical conductivity, mechanical properties, and wettability of the scaffold were studied. The biocompatibility of the scaffold was evaluated by assessing the adhesion and proliferation of mouse osteoblast MC3T3-E1 cells and *in vitro* degradability. It was found that the fabricated scaffold can be considered as a prospective candidate for bone tissue engineering applications.

EXPERIMENTAL

Materials

Tris(methylol)propane (TMP), 2,2-*bis*(methylol)propionic acid (*bis*-MPA), and *p*-toluenesulfonic acid (*p*-TSA) were purchased from Fluka (USA), and were used as received. Poly(ϵ-caprolactone) (PCL) (M_n = 70,000–90,000 g mol^{-1}), tetraethylammonium tetrafluoroborate (TEAFB), anhydrous ferric chloride ($FeCl_3$), 2-thiopheneacetic acid, *N*,*N*-dicyclohexyl carbodiimide (DCC), and *N*-hydroxysuccinimide (NHS) were purchased from Sigma-Aldrich (USA), and were used as received. Thiophene monomer was purchased from Merck (Darmstadt, Germany), and was distilled twice under reduced pressure before use. All other reagents were purchased from Merck and purified according to standard methods.

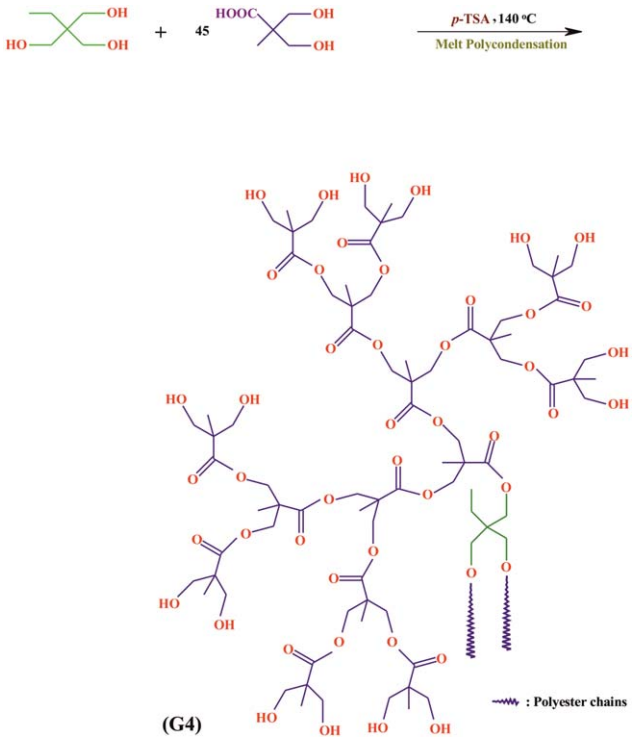

SCHEME 1. Synthesis of hyperbranched aliphatic polyester (G4).

Synthesis of hyperbranched aliphatic polyester (HAP; G4)

A three-necked round-bottom flask equipped with a stirrer, condenser, and thermometer was charged with a mixture of TMP (0.745 g, 5.55 mmol), *bis*-MPA (6.71 g, 50.0 mmol) (in stoichiometric correspondence to a perfect second generation), and a catalytic amount of *p*-TSA (0.05 g, 0.28 mmol). The reaction mixture was heated for about 3 h at 140 ± 3°C under a stream of argon gas, with removing the water formed during the reaction. At the end of this time, the *bis*-MPA corresponding to the third generation (8.94 g, 66.7 mmol), and *p*-TSA (0.05 g, 0.28 mmol) were added and the argon flow was started. The reaction mixture was heated for about 3 h at 140 ± 3°C under a stream of argon gas, with removing the water formed during the reaction. Afterwards, the *bis*-MPA corresponding to the fourth generation (17.85 g, 133.3 mmol), and *p*-TSA (0.05 g, 0.28 mmol) were added and the argon flow was started. The reaction mixture was heated for about 3 h at 140 ± 3°C under a stream of argon gas, with removing the water formed during the reaction. At the end of this time, a glass-like product (defined as G4) was obtained. The crude product was dissolved in tetrahydrofuran (THF) and precipitated in excess methanol, in order to remove residual monomers and catalyst. The product was filtered, washed several times with methanol, and dried in vacuum at room temperature (Scheme 1).

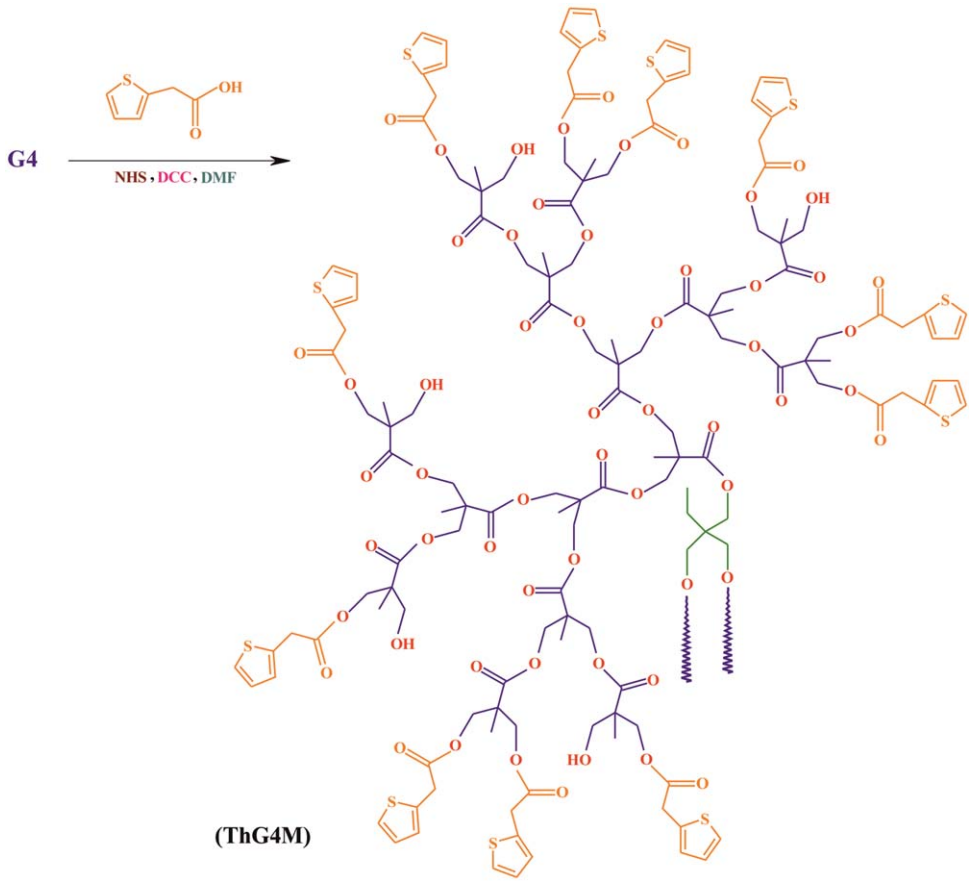

SCHEME 2. Synthesis of the thiophene-functionalized G4 macromonomer (ThG4M).

Synthesis of thiophene-functionalized G4 macromonomer (ThG4M)

A 250 mL three-necked round-bottom flask equipped with condenser, gas inlet/outlet, and a magnetic stirrer, was charged with 2-thiopheneacetic acid (3.82 g, 27 mmol), DCC (30 mmol, 6.20 g), NHS (3.45 g, 30 mmol), and dried *N*,*N*-dimethylformamide (DMF; 100 mL). The reaction mixture was deaerated by bubbling highly pure argon for 15 min, and stirred magnetically at room temperature for about 6 h under an argon atmosphere. At the end of this time, the reaction mixture was filtered using filter paper (Whatman) to remove dicyclohexyl urea salts as the by-product. Afterward, the G4 (3.0 g, 1.2 mmol) was added to the above mentioned solution, and the reaction mixture was stirred for another 24 h at room temperature under an argon atmosphere. The ThG4M macromonomer was separated by precipitation in excess methanol (300 mL), filtered, washed several times with methanol, and dried in vacuum at room temperature (Scheme 2).

Synthesis of G4-PTh via chemical oxidation polymerization method

A 100 mL three-necked round-bottom flask equipped with a condenser, dropping funnel, gas inlet/outlet, and a magnetic stirrer, was charged with ThG4M (1.0 g, 0.235 mmol), and dried $CHCl_3$ (90 mL). The mixture was refluxed at 65°C for about 1 h to completely dissolve the macromonomer. At the end of this time, the flask was cooled to room temperature, added thiophene monomer (3 mL, 38.2 mmol), and then the reaction mixture was deaerated by bubbling highly pure argon for 10 min.

In a separate container 24.8 g (153 mmol) of anhydrous ferric chloride was dissolved in 30 mL of dried acetonitrile. This solution was deaerated by bubbling highly pure argon for 10 min, and then slowly added to the reaction mixture at a rate of 5 mL min^{-1} under an argon atmosphere. The reaction mixture was refluxed for about 24 h at room temperature under an inert atmosphere. The reaction was terminated by pouring the contents of the flask into a large amount of methanol. The product was filtered, and washed several times with methanol. The final dark red solid was dried in vacuum at room temperature. The crude product was extracted with THF in a Soxhlet apparatus for 24 h, in order to remove pure PTh. The synthesized G4-PTh is soluble in hot THF, while pure PTh is not soluble in this solvent (see Table I). The polymer solution was filtered, precipitated into excess methanol, and dried in reduced pressure to give a dark red powder.

The homopolythiophene (H-PTh) was synthesized by the same method, in the absence of the ThG4M macromonomer.

Electrospinning of the G4-PTh and PCL

The G4-PTh/PCL nanofibers were prepared by subsequent electrospinning the same volume solutions of G4-PTh (1% w/v), and PCL (3% w/v) under conditions described in our previous works.[30,31]

Biocompatibility analysis

Cell culture. The mouse osteoblast cells (MC3T3-E1 cell line) was cultured into flasks, and kept in a humidified incubator with 5% CO_2 at 37°C. The cells were grown in the Dulbecco's modified Eagle's medium (DMEM; Sigma-Aldrich, USA) with 10% (v/v) fetal bovine serum (FBS), and antibiotics (100 mg mL^{-1} penicillin–streptomycin).

Cell viability assay. MTT assay was applied to evaluate the cytotoxic effect of the G4-PTh/PCL electrospun nanofibers. The mouse osteoblast MC3T3-E1 cells were seeded in 96 well plates, and allowed to attach overnight and then were treated with nanofibers. The nanofibers were sterilized using gamma radiation prior to the cell viability experiment. After incubation for about 48 h, 50 mL of the MTT reagent (2 mg mL^{-1} in phosphate-buffered saline; PBS, pH 7.4; Invitrogen, CA, USA) was added to each well, and incubated at 37°C for another 4 h in a humidified CO_2 incubator. At the end of this period, the formazan crystals were dissolved in DMSO and the UV absorbance was measured at 570 nm using a spectrophotometric plate reader, ELx 800 (Biotek, San Francisco, CA, USA).

Cell growth assay. The direct counting by hemocytometer was employed for evaluating of cell growth rate. Briefly, the cells were poured on to the precoated well with electrospun nanofibers at a seeding density of 1×10^5 cells per cm^2. The medium was added to each well, and were incubated for 7 days at 37°C in an atmosphere of 5% CO_2 with medium exchanges every 2 days. The cells were detached by trypsinization, and further trypsin was deactivated using more media. Finally, 10 μL of cell sample were mixed by trypan blue (1:1 v/v), and then the clear blue viable cells were counted using hemocytometer slide.

Cell morphology study. The morphologies of the adhered mouse osteoblast MC3T3-E1 cells on to G4-PTh/PCL electrospun nanofibers was studied by means of scanning electron microscopy (SEM). Briefly, six-well plates were precoated with nanofibers, and mouse osteoblast MC3T3-E1 cells were then seeded (5×10^4 cells per well) on plates. After 24 h, the cells were fixed with 2% glutaraldehyde (Sigma-Aldrich, USA) for 1 h at room temperature, and the morphologies of the cells were observed by means of SEM.

Characterization

Fourier transform infrared (FTIR) spectra of the samples were collected on a Shimadzu 8101M FTIR (Shimadzu, Kyoto, Japan) between the wavenumber range of 4000 to 400 cm^{-1}. The samples were prepared by grinding the dry powders with potassium bromide (KBr), and compressing the mixture into disks. The spectra were recorded at room temperature. The ^1H nuclear magnetic resonance (NMR) spectra of the samples were recorded at 25°C using an FT-NMR (400 MHz) Bruker spectrometer (Bruker, Ettlingen, Germany). The sample for NMR spectroscopy was prepared by dissolving about 10 mg of sample in 1 mL of deuterated dimethylsulfoxide (DMSO-d_6) or deuterated chloroform ($CDCl_3$), and chemical shifts were reported in parts per million (ppm) units with tetramethylsilane (TMS) as internal standard. The field emission scanning electron microscope (FE-SEM) type 1430 VP (LEO Electron Microscopy, Cambridge, UK) was applied to determine the morphologies of the samples. Thermal properties of the samples were examined by thermogravimetric analyzer [TGA-PL STA 1640 equipment (Polymer Laboratories, Shropshire, UK)]. The TGA experiments were conducted under nitrogen atmosphere in a temperature range of 25–700°C with heating rate of 10°C min^{-1}. Electrochemical experiments were conducted using Auto-Lab PGSTA T302N. The electrochemical cell contained five openings: three of them were used for the electrodes (working, counter, and reference), and two for argon bubbling in the solutions during all experiments. The conductivities of the synthesized samples were determined using the four-probe technique (Azar Electrode, Urmia, Iran) at room temperature. The ultimate tensile strength and strain to break were determined using a Zwick tensile testing machine (Z 010, Zwick/Roell, Ulm, Germany). The wettability of the electrospun nanofibers were investigated by drop water contact angle measurement using an OCA 20 plus contact angle meter system (DataPhysics Instruments GmbH, Filderstadt, Germany). The droplet size was 5 μL, and at least five samples were used for each test.

RESULTS AND DISCUSSION

It is well known that the polythiophene (PTh) is capable of high charge carrier mobilities without charge traps in grain boundaries. This property is originated from its extended planar π-conjugated and interdigitated intermolecular ordering. Thus, PTh can be incorporated in various practical, technological as well as biomedical applications. Among the biomedical applications of PTh tissue regeneration based on biocompatible materials of this conducting polymer is of particular interest. In addition, the biocompatibility, physical properties, and chemical composition of the tissue engineering scaffolds are the most important factors, since these affects cell attachment, proliferation, migration, differentiation, and neo-tissue formation.[13,32,33] The overall methodology for the fabrication of biocompatible, porous, and electrically conductive scaffold for regenerative medicine is shown in Scheme 3.

Characterization of ThG4M macromonomer

The FTIR spectra of the G4 and ThG4M macromonomer are illustrated in Figure 1. The FTIR spectrum of the G4 shows the characteristic absorption bands due to the stretching vibrations of aliphatic C–H at 2950 to 2800 cm^{-1} region, stretching vibration of carbonyl group at 1722 cm^{-1}, C—H bending vibrations at 1377 and 1464 cm^{-1}, and C—O stretching vibrations at 1036 and 1207 cm^{-1}. Furthermore,

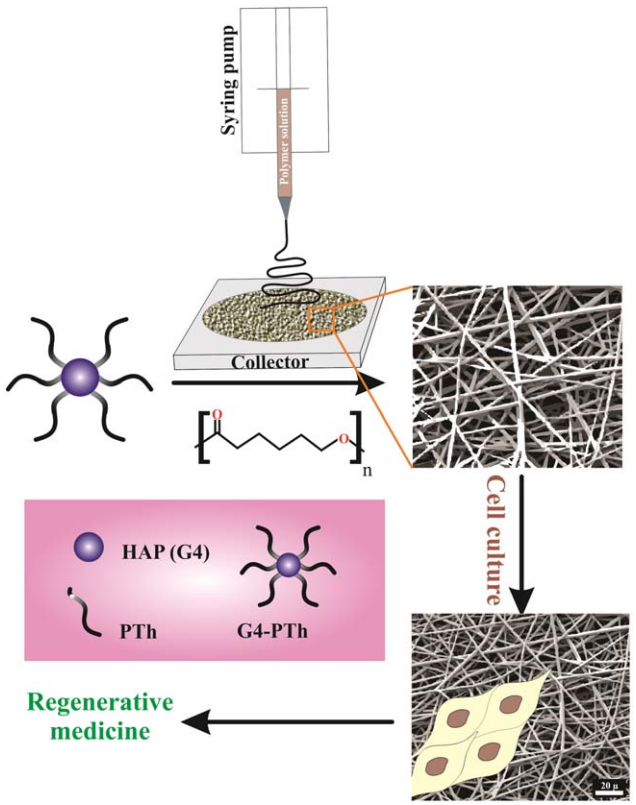

SCHEME 3. The overall methodology for the fabrication of biocompatible, porous, and electrically conductive scaffold for regenerative medicine.

the hydroxyl end groups appeared as a broad strong band centered at 3404 cm^{-1}.

The successful synthesis of the ThG4M is verified by the appearance of new bands as follows: the stretching vibrations of aliphatic and aromatic C—H at 3100 to 2800 cm^{-1} region, γ(C—H) in the aromatic ring at 697 and 785 cm^{-1}, unreacted hydroxyl end groups as a broad strong band centered at 3408 cm^{-1}, and the aromatic C═C stretching vibration at 1573 cm^{-1}. In addition, the band at 1635 cm^{-1} may be related to the carbonyl stretching vibration of 2-thiopheneacetate group.

The synthesized ThG4M macromonomer was further characterized by means of ^{1}H NMR spectroscopy. Figure 2, shows the ^{1}H NMR spectra of the G4, and ThG4M macromonomer. In ^{1}H NMR spectrum of the G4 the unreacted linear, and terminal hydroxyl groups (OH_L and OH_T, respectively) appeared at 4.85, and 4.45 ppm, respectively. The chemical shifts at 4.05 and 3.35 ppm are related to the CH_2OR (OR: reacted; i.e., OH), and CH_2OH (overlapped with H_2O), respectively. The chemical shifts at 0.90 to 1.35 ppm are corresponded to the methylene, and methyl groups in this sample. In addition, the chemical shifts at 2.50 and 3.33 ppm assigned to the H_2O and dimethyl sulfoxide (as impurities in NMR solvent), respectively. The successful synthesis of the ThG4M is verified by the appearance of new chemical shifts at 3.10 and 6.85 to 7.25 corresponding to —CH_2, and thiophene ring protons of the 2-thiopheneacetate groups, respectively.

In the past few decades ^{1}H NMR spectroscopic analysis has been established as a powerful tool for the determination of some parameters of polymers such as compositions, degree of polymerizations (DP_n), and number average molecular weight (M_n). The DP_n and M_n of the synthesized polyester (G4) can be calculated from the ^{1}H NMR data through the following equations.

$$\mathrm{DP_n} = 3I_A/I_{CH3,TMP}$$
$$I_A = (I_{CH2OR} + 2[I_{(OH)L} + I_{(OH)T}] - 4I_{CH3,TMP})/4$$
$$M_n = M_{TMP} + \mathrm{DP}_n \times (M_{Bis-MPA} - M_{H_2O})$$

where I_i indicates integral intensity of protons i in the ^{1}H NMR spectrum. According to ^{1}H NMR data, the DP_n and M_n were calculated to be 19.76, and 2428 g mol^{-1}, respectively.

In addition, the 2-thiopheneacetate content in the synthesized macromonomer was calculated through the following equation. Thus, the M_n of ThG4M is 4254 g mol^{-1}, and 74% of the hydroxyl groups were converted to 2-thiopheneacetate groups.

$$n_{Th} = \frac{I_{(Th)}/3}{\frac{[I_{(CH2OR)} + I_{(CH2OH)}]/4}{DP_{n,\ G4}}} = 14.73$$

Synthesis of G4-PTh

The FTIR spectra of the synthesized H-PTh and G4-PTh are shown in Figure 3. The most important bands in the

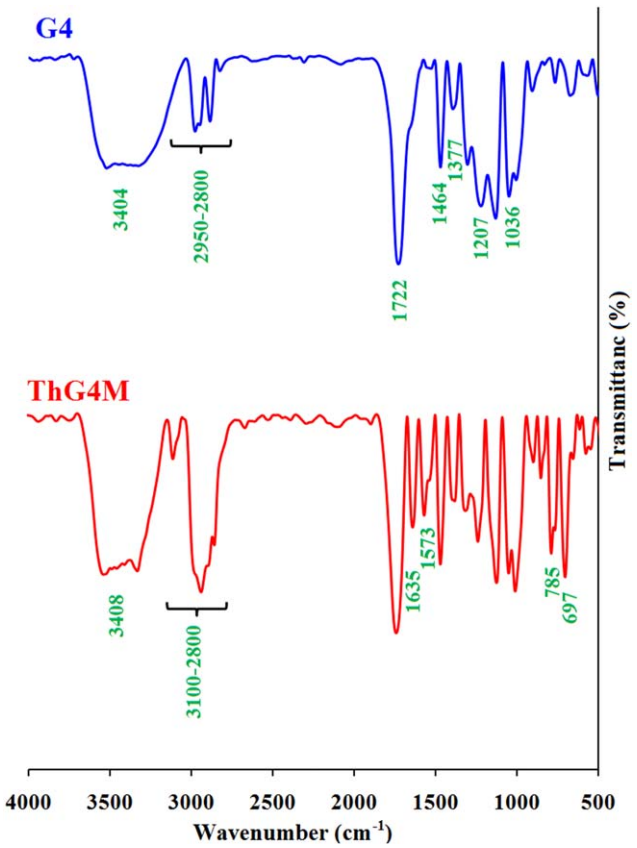

FIGURE 1. The FTIR spectra of the G4 and ThG4M macromonomer.

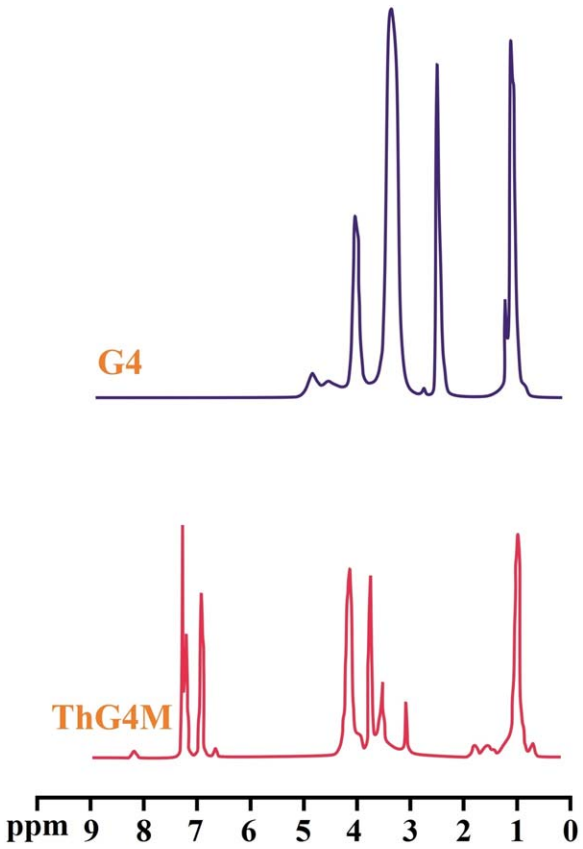

FIGURE 2. The ^{1}H NMR spectra of the G4 (in DMSO-d_6), and ThG4M (in $CDCl_3$).

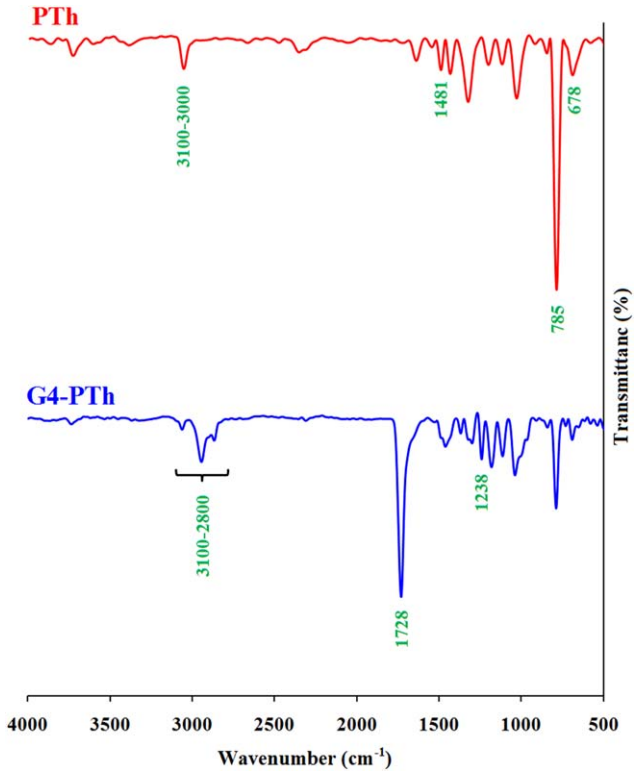

FIGURE 3. The FTIR spectra of the H-PTh, and G4-PTh.

FTIR spectrum of the H-PTh can be listed as follows: weak aromatic α and β hydrogen's of thiophene ring at 3100 to 3000 cm^{-1} region, γ(C—H) in the aromatic ring at 785 cm^{-1}, the aromatic C═C stretching vibration at 1481 cm^{-1}, and the C—S stretching vibration at 678 cm^{-1}. The successful grafting of the PTh onto ThG4M is verified by the appearance of new bands such as stretching vibration of carbonyl group at 1728 cm^{-1}, C—O stretching vibration at 1238 cm^{-1}, and the stretching vibrations of aliphatic and aromatic C—H at 3100–2800 cm^{-1} region.

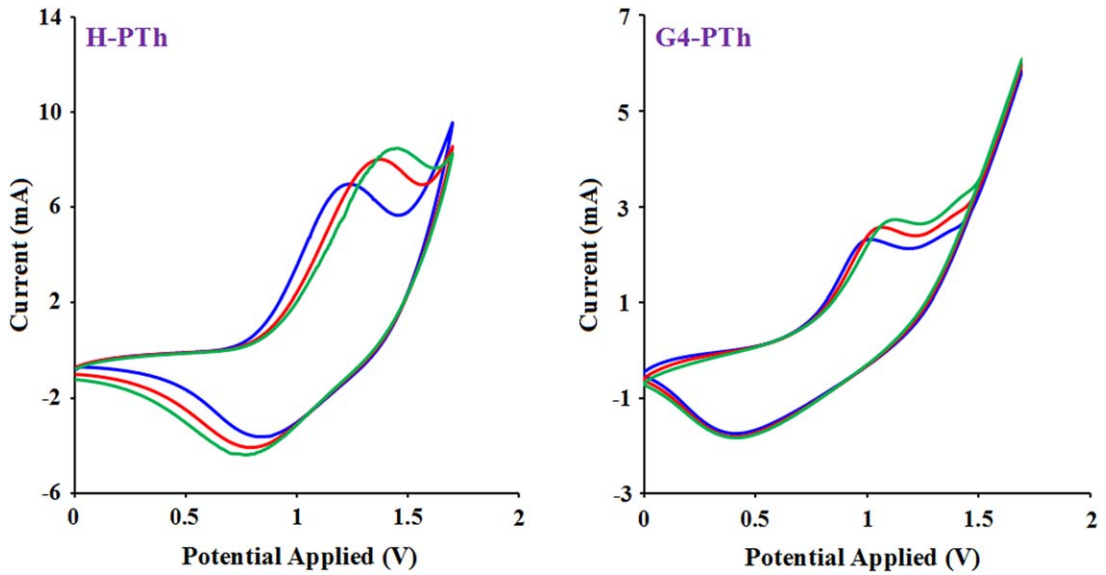

FIGURE 4. Cyclic voltammetry curves (CVs) of the H-PTh and G4-PTh samples in a acetonitrile–tetraethylammonium tetrafluoroborate (TEAFB), solvent–electrolyte couple (0.1 mol L^{-1}) (blue cycle 10 mV s^{-1}; red cycle 20 mV s^{-1}; and green cycle 30 mV s^{-1}).

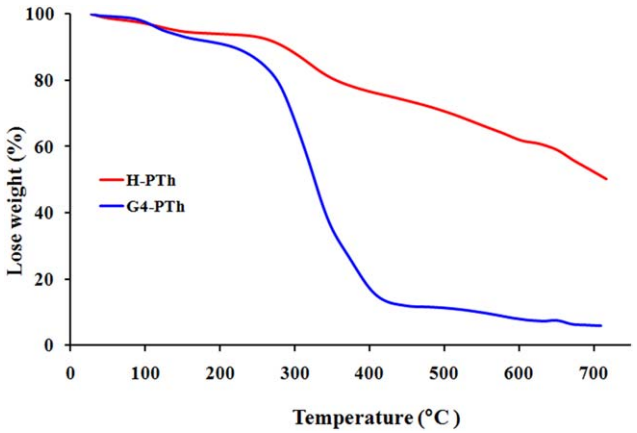

FIGURE 5. The TGA curves of the G4-PTh, and H-PTh samples.

Electroactivity behaviors

It is well demonstrated that electrical signals can regulate cell attachment, proliferation, and differentiation. Thus, the electric fields and stimulations are very helpful for wound healing, repair of the damaged spin cord, and nerve regeneration.[34–36] Base on these reasons, the electrically conductive scaffolds are the best and first choose in the field of regenerative medicine.

The electroactivity behaviors of the H-PTh and G4-PTh were studied under cyclic voltammetric (CV) conditions in the range of 10–30 mV s^{-1} scan rate, in the acetonitrile–tetraethylammonium tetrafluoroborate (TEAFB), solvent–electrolyte couple (0.1 mol L^{-1}) between 0 and +1.70 V versus the reference electrode (Ag/AgCl) under argon protection (Fig. 4). The H-PTh shows a typical redox couple with anodic and cathodic peaks at approximately 1.35, and 0.77 V versus Ag/AgCl electrode, respectively. In contrast, as shown in Figure 4, the typical CVs of the G4-PTh exhibited some qualitative similarities to those of the H-PTh. This sample shows a typical redox couple with anodic and cathodic peaks at approximately 1.10, and 0.42 V versus Ag/AgCl electrode, respectively. In addition, in both samples the anodic peaks shift in the direction of positive potential with increasing scan rate. This indicates the electrochemical oxidation/reduction (doping/dedoping) of H-PTh, and G4-PTh samples were chemically reversible.

TABLE I. Solubility of G4-PTh, Pure PTh, and G4 in Common Organic Solvents[a]

Solvent	Xylene	$CHCl_3$	THF	DMF	NMP	DMSO
PTh	–	–	–	+	+	+
G4	–	+	+++	+++	+++	+++
G4-PTh	–	–	++	+++	+++	+++

[a] +++: soluble; ++: sparingly soluble; +: slightly soluble; –: insoluble; the concentration used in the solubility test was 10 mg of each polymer in 1 mL of solvents at room temperature (DMSO, dimethylsulfoxide; NMP, *N*-methylpyrrolidone; THF, tetrahydrofuran; DMF, *N*,*N*-dimethylformamide).

Thermal property study

The thermal stability of the G4-PTh, and H-PTh upon heating in nitrogen atmosphere were investigated by means of TGA. As seen in Figure 5, the thermal decomposition of the G4-PTh is started from 250°C, and the weight loss increases rapidly from this temperature to about 420°C, after which the loss rate slows down. The residue at 700°C for this sample is 6 wt %. In contrast, the thermal decomposition of the H-PTh is started from 280°C, and the weight loss increases rapidly from this temperature to about 700°C. The residue at 700°C for H-PTh is 48 wt %. It is important to note that the weight loss of the both samples between 100 and 200°C

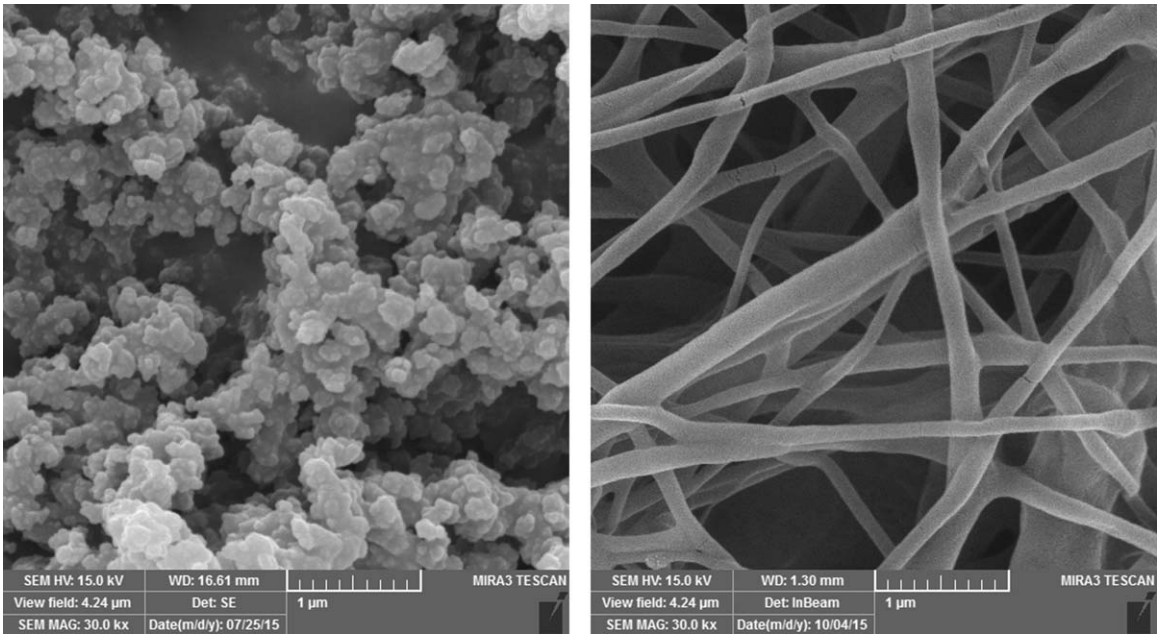

FIGURE 6. The FE-SEM images of the G4-PTh (left), and G4-PTh/PCL electrospun nanofibers (right).

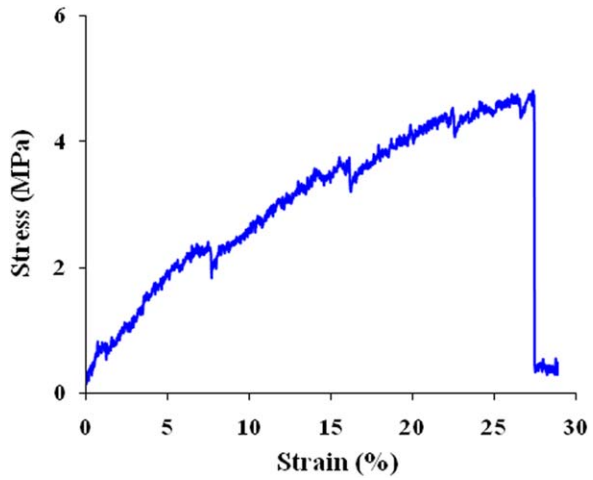

FIGURE 7. The stress–strain curve of the G4-PTh/PCL electrospun nanofibers.

is related to the evaporation of residual water or organic solvents in the samples.

Solubility test

As known the main drawback of nonsubstituted PTh is the poor processability both in melt and solution processing. In this respect, an efficient and versatile approach is the synthesis of PTh copolymers with processable polymers (e.g., polyesters).[17–19] The solubility of the G4-PTh, pure PTh, and polyester (G4) in common organic solvents are summarized in Table I. As seen in this table the solubility of G4-PTh in common organic solvents improved significantly compared to pure PTh.

Characterization of electrospun nanofibers

The design and development of biocompatible and electrically conductive polymers is an important field for biomedical applications. In this regard, the electrospinning is an efficient, versatile, simple, and quick approach for fabricating biodegradable and electrically conductive nonwoven mats of nanofibers for biomedical applications, such as regenerative medicine. This process is based on the application of a strong electrostatic field between a capillary, connected to a tank containing a polymer solution, and a ground collector. It is well established that the polymeric nanofiber scaffolds can mimic the architecture and biological functions of the ECM.[37,38]

Morphology study. The surface morphologies of the G4-PTh (Fig. 6; left), and G4-PTh/PCL electrospun nanofibers (Fig. 6; right) were observed by means of FE-SEM. As seen in Figure 6, the G4-PTh exhibits the porous and nanostructured morphology with an average diameter of 100 ± 20 nm. This morphology may be originated from the growth of the PTh from ThG4M macromonomer. The SEM image of the G4-PTh/PCL electrospun nanofibers indicated the three-dimensional interconnected pore structure, with an average diameters in the size range of 100 ± 40 nm were formed for electrospun nanofibers.

Mechanical properties of nanofibers. The mechanical properties of the polymeric nanofiber scaffold are very important factors in its performance. Because the mechanical properties of the nanofibers influence the cell interaction during culture, and thus cellular adhesion, proliferation, and signaling. Furthermore, the elasticity of the scaffold affected the cellular activities such as neurite extension, cell spreading, and differentiation.[39,40] Thus, the well characterization of mechanical properties is an important step in the fabricating of scaffolds for regenerative medicine.

The representative mechanical property of the G4-PTh/PCL electrospun nanofibers is shown in Figure 7. The Young's modulus, tensile strength, and elongation at break were obtained to be 59.81 ± 7.4 (MPa), 4.81 ± 1.7 (MPa), and 27.79 ± 6.8 (%), respectively.

Hydrophilicity and degradability of nanofibers. A biomaterial as *in vivo* tissue engineering scaffold has a direct contact with blood, therefore its surface properties is a very

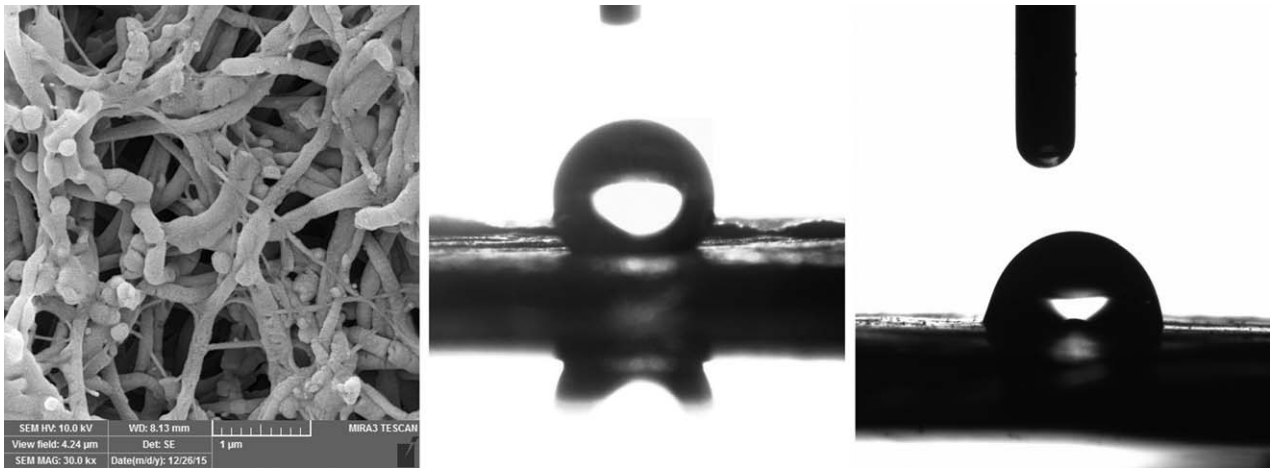

FIGURE 8. The FE-SEM image of the G4-PTh/PCL electrospun nanofibers after 15 days soaking in PBS (left), and the photographs of water drops on PCL (center), and G4-PTh/PCL (right) electrospun nanofibers.

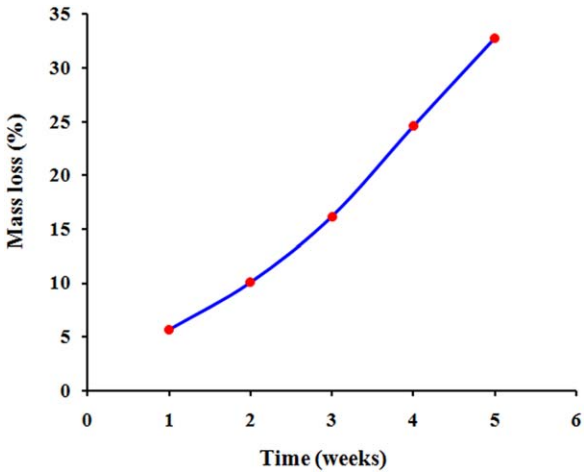

FIGURE 9. Degradation profile of the G4-PTh/PCL electrospun nanofibers.

important factor, and can affected the behavior of seeded cells. In this context, the wettability, and degradability of the scaffolds are important properties, which could influence their performance such as extent of protein adsorption and cell attachment.

The drop water contact angles of the G4-PTh/PCL and pure PCL electrospun nanofibers were measured at room temperature to investigate the surface properties of the nanofibers. The contact angles of G4-PTh/PCL and PCL electrospun nanofibers with water were calculated to be 94° ± 3.1° and 136° ± 2.6°, respectively. In addition, the photographs of water drops on G4-PTh/PCL and PCL electrospun nanofibers are shown in Figure 8.

Un-degradable polymers could result in chronic inflammation due to their long stay in the body, thus the biodegradation of scaffold is a critical feature. In addition, the biodegradation of scaffold is beneficial to enable tissue integration, and to avoid subsequent surgical removal of scaffold. The *in vitro* degradability of the G4-PTh/PCL electrospun nanofibers was examined through evaluating the morphological change, and gravimetric measurements after soaking the nanofibers in phosphate-buffered saline (PBS; pH 7.4; Invitrogen, CA, USA) at 37°C. The PBS was updated every five days. After reaching the designed time, the specimens were retrieved, washed several times with double distilled water, dried in reduced pressure, and then weighed. The mass loss percentage was calculated from: $(W_i - W_r)/W_i$;where W_i and W_r are the initial and the residual dry weights of the electrospun nanofibers. As shown in Figure 9, the electrospun nanofibers has a fast mass loss up to five weeks with a linear degradation trend. After 5 weeks, the mass loses for G4-PTh/PCL was obtained to be 32.8 wt %.

In addition, the FE-SEM image of the sample after 15 days soaking in PBS showed that the G4-PTh/PCL electrospun nanofibers are undergoing to swelling and degradation (Fig. 8).

TABLE II. Electrical Properties of the Samples

Sample	Volume Specific Resistivity (ρ; Ω cm)	Electrical Conductivity (σ; S cm^{-1})
H-PTh	1.23	0.81
G4-PTh	1.56	0.64
G4-PTh/PCL[a]	143	0.007

[a]The G4-PTh/PCL electrospun nanofibers were provided as given in "Experimental" section.

Electrical conductivity measurement

The electrical conductivity of scaffold plays an important role in controlling cell behavior, so the performance of the tissue engineering scaffold can be improved through increasing the electrical communication among the cells.[29,41]

The electrical conductivities (σ; S cm^{-1}) of the samples were measured by the standard four-probe technique at room temperature. The experimental determinations were repeated five times for each sample to evaluate the measurement accuracy. The conductivities were calculated from the following equations:

$$\rho = (V/I)\ (\pi/\ln 2)d$$
$$\sigma = 1/\rho$$

where V is the voltage, I is the current, d is the thicknesses, and ρ (Ω cm) is the volume specific resistivities of the samples. The electrical conductivities results obtained are summarized in Table II. As can be seen the G4-PTh exhibited the lower electrical conductivity than those of the H-PTh, mainly due to the decreased conjugation length distribution in the case of the G4-PTh sample. As expected, the electrical conductivity of the G4-PTh/PCL electrospun naofibers would be significantly decreased, since PCL is an insulating material. Despite, it is well established that the conductivity in the semiconductor range (10^{-5} S cm^{-1}) is sufficient for tissue engineering and other medical regenerative purpose.

On the basis of findings from electrical conductivity and electroactivity studies, the conclusion could be drawn that

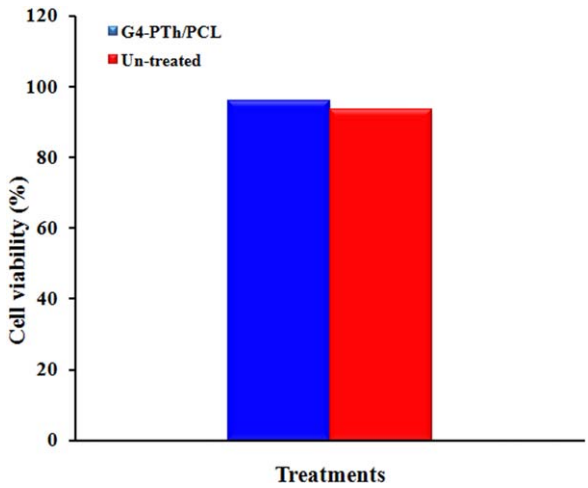

FIGURE 10. *In vitro* cytotoxicity effects of the G4-PTh/PCL electrospun nanofibers on mouse osteoblast MC3T3-E1 cells.

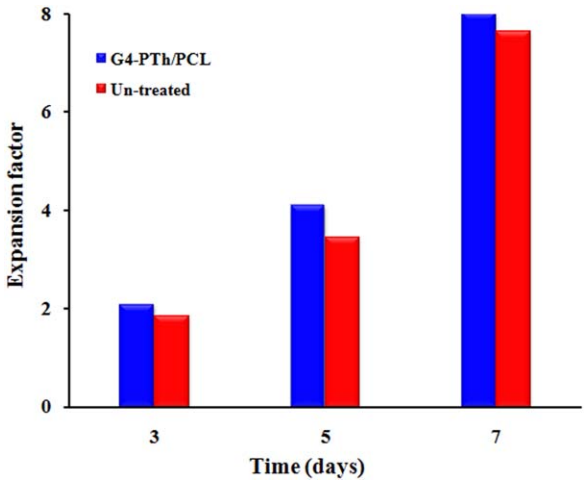

FIGURE 11. The mouse osteoblast MC3T3-E1 cells growth performance of the G4-PTh/PCL electrospun nanofibers.

the G4-PTh has lower electrical conductivity and electroactivity than those of the H-PTh. However, the lower electrical conductivity and electroactivity levels can be improved at the price of solubility, processability, and biocompatibility.

Biocompatibility

Cytotoxic effects of the electrospun nanofibers. The potential cytotoxic effect of the G4-PTh/PCL electrospun nanofibers was evaluated by means of MTT assay. The results showed that these electrospun nanofibers were not able to induce cytotoxicity in mouse osteoblast MC3T3-E1 cells (Fig. 10).

Cell growth assay. The biocompatibility of the tissue engineering scaffold is an important factor, since it can influence cell attachment, proliferation, migration, differentiation, and neo-tissue formation. The cell growth performance of the G4-PTh/PCL electrospun nanofibers surfaces were evaluated at the initial seeding densities of 1×10^5 cells per cm^2 using the mouse osteoblast MC3T3-E1 cell line (Fig. 11). The results showed that the osteoblast cells were expanded 8 ± 0.1 factor at the end of the cell culture period (7 days) on to the G4-PTh/PCL electrospun nanofibers. In contrast, nontreated cells were expanded 7.2 ± 0.2 factor at the same time of culture. Thus, the prepared G4-PTh/PCL electrospun nanofibers can be considered as a protective candidate for improve cells proliferation, mainly due to improve cellular interactions.

Cell morphology study. The morphological behavior and cellular adhesion are the most important parameters for evaluating the biocompatibility of any biomaterial, since it may directly affect the reproduction quality of the cells. Therefore, SEM images were used to evaluate cellular adhesion properties of the prepared nanofibers. Figure 12 shows the FE-SEM images of the mouse osteoblast MC3T3-E1 cells onto the G4-PTh/PCL electrospun nanofibers. The FE-SEM images exhibited that the osteoblast cells have sufficient cellular adhesion to the nanofibers.

CONCLUSION

A novel three-dimensional, conducting, biocompatible, and porous scaffold composed of hyperbranched aliphatic polyester, polythiophene, and poly(ε-caprolactone) for application in regenerative medicine has been successfully fabricated using the procedure developed in our laboratory. The some properties such as microstructures, mechanical characteristics, hydrophilicity, electrical conductivity, and electroactivity of the fabricated scaffold were examined, and

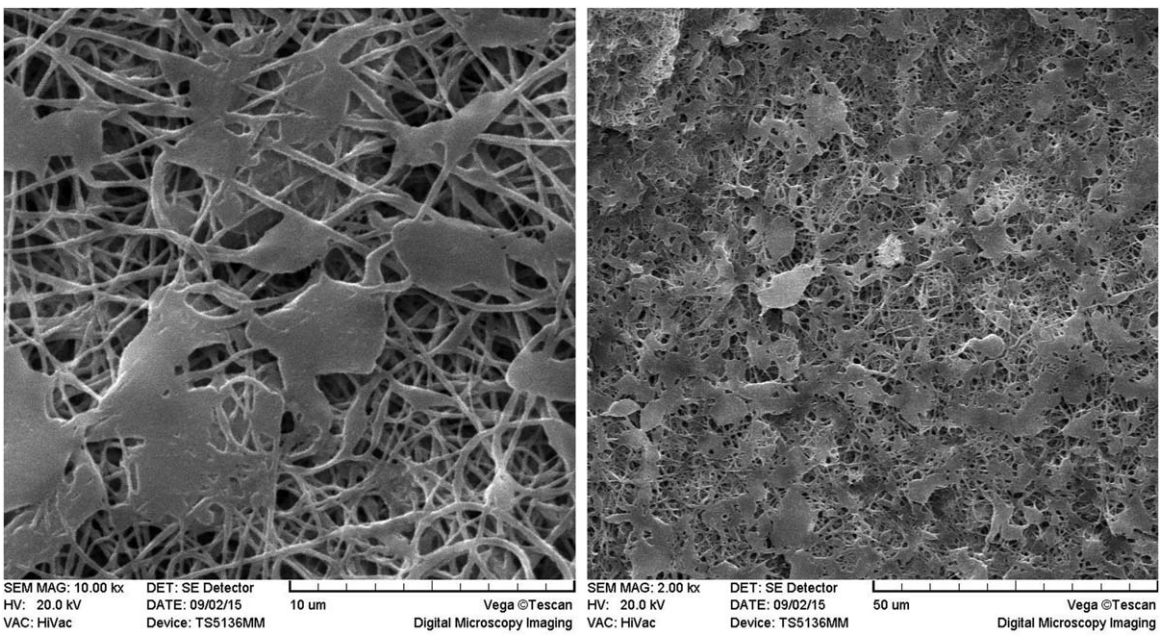

FIGURE 12. The SEM images of the mouse osteoblast MC3T3-E1 cells on to the G4-PTh/PCL electrospun nanofibers at different magnifications.

it was found that this scaffold can be considered as suitable material having proper conductivity, and mechanical properties that would be potentially used for tissue engineering. The biocompatibility of the fabricated scaffold was primarily investigated by assessing the adhesion and proliferation of mouse osteoblast MC3T3-E1 cells, and *in vitro* degradability. The biocompatibility analysis results showed that the prepared scaffold was not able to induce cytotoxicity in the mentioned cell line, and improved the cells proliferation. Based on finding, we envision that the fabricated scaffold can be used as a model system for understanding the role of electrical signals in proliferation and differentiation of verious cell lines. It would be expected that further studies will focused on the design and development of biocompatible and electrically conductive polymeric scaffolds, in order to control the electrochemical signals.

ACKNOWLEDGMENTS

We express our gratitude to the Payame Noor University, and Research Center for Pharmaceutical Nanotechnology, Tabriz University of Medical Sciences for supporting this project. Also, the authors sincerely thank Dr. Ali Baradar-Khoshfetrat, Sahand University of Technology, Tabriz, Iran for his valuable technical and equipment's cooperation's.

REFERENCES

1. Lutolf MP, Weber FE, Schmoekel HG, Schense JC, Kohler T, Müller R, Hubbell JA. Repair of bone defects using synthetic mimetics of collagenous extracellular matrices. Nat Biotechnol 2003; 21:513–518.
2. Carnemolla B, Borsi L, Balza E, Castellani P, Meazza R, Berndt A, Ferrini S, Kosmehl H, Neri D, Zardi L. Enhancement of the antitumor properties of interleukin-2 by its targeted delivery to the tumor blood vessel extracellular matrix. Blood 2002;99:1659–1665.
3. Cho C, Seo S, Park I, Kim S, Kim T, Hoshiba T, Harada I, Akaike T. Galactose-carrying polymers as extracellular matrices for liver tissue engineering. Biomaterials 2006;27:576–585.
4. Uppanan P, Thavornyutikarn B, Kosorn W, Kaewkong P, Janvikul W. Enhancement of chondrocyte proliferation, distribution, and functions within polycaprolactone scaffolds by surface treatments. J Biomed Mater Res A 2015;103:2322–2332.
5. Kim DH, Richardson-Burns SM, Hendricks JL, Sequera C, Martin DC. Effect of immobilized nerve growth factor on conductive polymers: Electrical properties and cellular response. Adv Funct Mater 2007;17:79–86.
6. Ghasemi-Mobarakeh L, Prabhakaran MP, Morshed M, Nasr-Esfahani MH, Baharvand H, Kiani S, Al-Deyab SA, Ramakrishna S. Application of conductive polymers, scaffolds and electrical stimulation for nerve tissue engineering. J Tissue Eng Regen Med 2011;5:e17–e35.
7. Yousefi AM, Hoque ME, Prasad RGSV, Uth N. Current strategies in multiphasic scaffold design for osteochondral tissue engineering: A review. J Biomed Mater Res A 2015;103:2460–2481.
8. Yazdimamaghani M, Razavi M, Mozafari M, Vashaee D, Kotturi H, Tayebi L. Biomineralization and biocompatibility studies of bone conductive scaffolds containing poly(3,4-ethylenedioxythiophene):poly(4-styrene sulfonate) (PEDOT:PSS). J Mater Sci Mater Med 2015;26:274.
9. Huang L, Hu J, Lang L, Wang X, Zhang P, Jing X, Wang X, Chen X, Lelkes PI, MacDiarmid AG, Wei Y. Synthesis and characterization of electroactive and biodegradable ABA block copolymer of polylactide and aniline pentamer. Biomaterials 2007;28:1741–1751.
10. Qazi TH, Rai R, Boccaccini AR. Tissue engineering of electrically responsive tissues using polyaniline based polymers: A review. Biomaterials 2014;35:9068–9086.
11. Sarvari R, Massoumi B, Jaymand M, Beygi-Khosrowshahi Y, Abdollahi M. Novel three-dimensional, conducting, biocompatible, porous, and elastic polyaniline-based scaffolds for regenerative therapies. RSC Adv 2016;6:19437–19451.
12. Mooney E, Mackle J, Blond D, O'Cearbhaill E, Shaw G, Blau W, Barry F, Barron V, Murphy J. The electrical stimulation of carbon nanotubes to provide a cardiomimetic cue to MSCs. Biomaterials 2012;33:6132–6139.
13. Niu X, Rouabhia M, Chiffot N, King MW, Zhang Z. An electrically conductive 3D scaffold based on a nonwoven web of poly(l-lactic acid) and conductive poly(3,4-ethylenedioxythiophene). J Biomed Mater Res A 2015;103:2635–2644.
14. Guimard NK, Gomez N, Schmidt CE. Conducting polymers in biomedical engineering. Prog Polym Sci 2007;32:876–921.
15. Rincon C, Chen CC, Meredith JC. Effect of poly (3-octylthiophene) doping on the attachment and proliferation of osteoblasts. Macromol Biosci 2010;10:1536–1543.
16. Li DF, Wang HJ, Fu JX, Wang W, Jia XS, Wang JY. Preparation of a hydrophobic polythiophene film to improve protein adsorption and proliferation of PC12 cells. J Phys Chem B 2008;112:16290–16299.
17. Jaymand M, Hatamzadeh M, Omidi Y. Modification of polythiophene by the incorporation of processable polymeric chains: Recent progress in synthesis and applications. Prog Polym Sci 2015;47:26–69.
18. Hatamzadeh M, Jaymand M, Massoumi B. Graft copolymerization of thiophene onto polystyrene synthesized via nitroxide-mediated polymerization and its polymer−clay nanocomposite. Polym Int 2014;63:402–412.
19. Massoumi B, Farnoudian-Habibi A, Jaymand M. Chemical and electrochemical grafting of polythiophene onto poly(vinyl chloride): Synthesis, characterization, and materials properties. J Solid State Electrochem 2016;20:489–497.
20. Heeger AJ. Semiconducting polymers: the third generation. Chem Soc Rev 2010;39:2354–2371.
21. Runge MB, Dadsetan M, Baltrusaitis J, Ruesink T, Lu L, Windebank AJ, Yaszemski MJ. Development of electrically conductive oligo(polyethylene glycol) fumarate-polypyrrole hydrogels for nerve regeneration. Biomacromolecules 2010;11:2845–2853.
22. Planellas M, Pérez-Madrigal MM, Del Valle LJ, Kobauri S, Katsarava R, Alemán C, Puiggalí J. Microfibres of conducting polythiophene and biodegradable poly(ester urea) for scaffolds. Polym Chem 2015;6:925–937.
23. Balint R, Cassidy NJ, Cartmell SH. Conductive polymers: Towards a smart biomaterial for tissue engineering. Acta Biomater 2014; 10:2341–2353.
24. Malmstrom E, Johansson M, Hult A. Hyperbranched aliphatic polyesters. Macromolecules 1995;28:1698–1703.
25. Qiu T, Tang L, Fu Z, Tuo X, Li Y, Liu D, Yang W. Modification of end-groups of aliphatic hyperbranched polyester. Polym Adv Technol 2004;15:65–69.
26. Zhang H, Patel A, Gaharwar AK, Mihaila SM, Iviglia G, Mukundan S, Bae H, Yang H, Khademhosseini A. Hyperbranched polyester hydrogels with controlled drug release and cell adhesion properties. Biomacromolecules 2013;14:1299–1310.
27. Zagar E, Zigon M. Aliphatic hyperbranched polyesters based on 2,2-*bis*(methylol)propionic acid—Determination of structure, solution and bulk properties. Prog Polym Sci 2011;36:53–88.
28. Jang YI, An BK. Hyperbranched polyester copolymers for thermal printing papers: The effects of alkyl chain units in the polymer backbone on developing capability. Polymer 2015;78:193–201.
29. Rad AT, Ali N, Kotturi HSR, Yazdimamaghani M, Smay J, Vashaee D, Tayebi L. Conducting scaffolds for liver tissue engineering. J Biomed Mater Res A 2014;102:4169–4181.
30. Massoumi B, Davtalab S, Jaymand M, Entezami AA. AB_2 Y-shaped miktoarm star conductive polyaniline-modified poly(ethylene glycol) and its electrospun nanofiber blend with poly(ε-caprolactone). RSC Adv 2015;5:36715–36726.
31. Massoumi B, Aali N, Jaymand M. Novel nanostructured star-shaped polyaniline derivatives and their electrospun nanofibers with gelatin. RSC Adv 2015;5:107680–107693.
32. Li Q, Ma L, Gao C. Biomaterials for *in situ* tissue regeneration: Development and perspectives. J Mater Chem B 2015;3:8921–8938.

33. Yang S, Leong KF, Du Z, Chua CK. The design of scaffolds for use in tissue engineering. Part I. Traditional factors. Tissue Eng 2001; 7:679–689.
34. Meng S. Nerve cell differentiation using constant and programmed electrical stimulation through conductive nonfunctional graphene nanosheets film. Tissue Eng Regen Med 2014;11:274–283.
35. Hughes BW, Kusner LL, Kaminski HJ. Molecular MD, architecture of the neuromuscular junction. Muscle Nerve 2006;33:445–461.
36. Kai D, Prabhakaran MP, Jin G, Ramakrishna S. Polypyrrole-contained electrospun conductive nanofibrous membranes for cardiac tissue engineering. J Biomed Mater Res A 2011;99:376–385.
37. Zhang YZ, Su B, Venugopa J, Ramakrishna S, Lim CT. Biomimetic and bioactive nanofibrous scaffolds from electrospun composite nanofibers. Int J Nanomed 2007;2:623–638.
38. Khajavi R, Abbasipour M, Bahador A. Electrospun biodegradable nanofibers scaffolds for bone tissue engineering. J Appl Polym Sci 2016;133:42883.
39. Gilbert PM, Havenstrite KL, Magnusson KEG, Sacco A, Leonardi NA, Kraft P, Nguyen NK, Thrun S, Lutolf MP, Blau HM. Substrate elasticity regulates skeletal muscle stem cell self-renewal in culture. Science 2010;329:1078–1081.
40. Das RK, Gocheva V, Hammink R, Zouani OF, Rowan AE. Stress-stiffening-mediated stem-cell commitment switch in soft responsive hydrogels. Nat Mater 2016;15:318–325.
41. Baheiraei N, Yeganeh H, Ai J, Gharibi R, Ebrahimi-Barough S, Azami M, Vahdat S, Baharvand H. Preparation of a porous conductive scaffold from aniline pentamer-modified polyurethane/PCL blend for cardiac tissue engineering. J Biomed Mater Res A 2015;103:3179–3187.